2022 IEEE International Conference on Robotics and Automation (ICRA)
May 23-27, 2022. Philadelphia, PA, USA

Design and Optimization of a Capture System for Precise UAV Landing on Disturbed Aquatic Surface Platforms

Chongfeng Liu[1,2], Zixing Jiang[1], Ruoyu Xu[1,2], Xiaoqiang Ji[2], Lianxin Zhang[1,2], Huihuan Qian[2,1,‡]

***Abstract*— In this paper, a new capture system for UAV precision landing in a disturbed environment is proposed. Compared with the traditional visual guided landing methods, perching mechanism based methods, and tethered landing methods, the proposed system takes into account the stability during landing process and retains the high accessibility of the UAV. The proposed system consists of a winch subsystem and a magnetic catcher device. They establish an automatic tethered-UAV system for landing before the UAV touchdown. We analyzed the design principle as well as the feasibility of the magnetic catcher. An optimization problem is formulated to obtain a better layout of magnets on the catcher. The problem is relaxed based on interpolation simulation of attraction force. Experiments are conducted both in indoor and outdoor environments based on different UAV platforms respectively. The results validate that the catcher design and the capture system can achieve a successful landing in both cases.**

I. INTRODUCTION

Unmanned Aerial Vehicle (UAV) is a typical robot system that has a wide spectrum of applications in the area of ocean tasks like filming [1], surveillance [2], search and rescue [3], and other missions [4]. The UAV is a good fit for these applications due to its ability to hover, to fly in very low altitudes and its high accessibility [5], However, the UAV landing is an inevitable and challenging task in these applications. Furthermore, a precise landing of a UAV that requires less landing space has advantages in UAV deployment because we could land more UAVs on the same size of the platform. On land, UAV landing is usually based on visual guidance to find a landing pad. Sometimes, when it needs a precise landing, researchers usually add some positioning mechanisms to align and fix the UAV. These mechanisms mainly include parallel pushers, "V" and "W-shaped" pushers, and cone-shaped funnels, these are, active and passive ways [6]. Also, perching mechanisms are studied by researchers [7], [8], [9], [10]. Unlike on land, the UAV landing in a water surface environment would be affected by external disturbances. It is apparent that a special procedure is required to safely and precisely land a UAV on a moving or shaking platform against external disturbances.

*This paper is partially supported by Project U1613226 and U1813217 supported by NSFC, China, from the Shenzhen Institute of Artificial Intelligence and Robotics for Society, the Shenzhen Science and Technology Innovation Commission, fundamental research grant KQJSCX20180330165912672 and PF.01.000143 from The Chinese University of Hong Kong, Shenzhen.

[1]School of Science and Engineering, The Chinese University of Hong Kong,Shenzhen.

[2]Shenzhen Institute of Artificial Intelligence and Robotics for Society, The Chinese University of Hong Kong, Shenzhen.

[‡]Corresponding author is Huihuan Qian, email: hhqian@cuhk.edu.cn

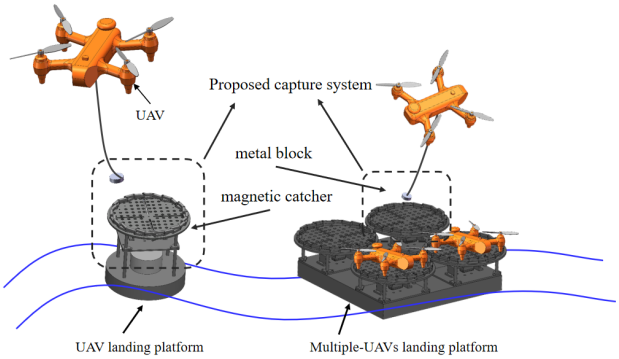

Fig. 1. The UAV releases down a suspended metal block to a magnetic catcher for landing. Based on the proposed capture system, the landing pad for the UAV occupies a small space, which makes it easy to implement a UAV array.

We can identify two mainstream approaches for the landing problem in disturbed occasions: i) free-flight landing based on tracking [11], ii) tethered-UAV landing methods [12]. The vision tracking method for UAV landing in disturbed environments is a classical approach that has been widely investigated and adopted [13], [14], [15]. In previous works, the landing was implemented where different controllers or tracking algorithms were applied to obtain a good landing point for UAV. It is conceivable that a precise UAV landing in a disturbed environment or a UAV landing on mobile platforms always require almost perfect tracking results, which require almost perfect predictions of the models. One of the best works of vision-guided landing was done by MIT researchers [16]. They conducted a successful landing of a UAV on a mobile platform with external turbulent wind conditions. The main drawback of this method is that it requires a large landing pad for UAV, since the touchdown positions do not keep the same in each landing. Such disadvantages also exist for the method of UAV perching. We can also get the information from previous work that the landing platform is always much larger than the UAV actual needs [11], [16]. Additionally, some small deviations from the optimal landing position may lead to a collision with the platform, or even a miss of landing may happen.

The tethered-guided UAV landing is another approach that is suitable for maritime occasions. This method uses a tether which links the UAV to a fixed point on the ground or deck of a ship [17]. In [18], researchers use the rope-driven method to realize the helicopter landing on the unmanned ship. Also, researchers in works like [19], [20], use the tether

together with an actuated winch to handle the problems of landing and takeoff on a flat moving platform for UAV. The previous works have shown the feasibility and stability of such a method in disturbed environments. This method has an advantage of precision UAV landing. However, the motion range and the maneuverability of the UAV are limited because of the limited length of the tether. And the tethers might become entangled when UAVs work in an array.

In this work, the challenge we are considering is performing a precision landing of a UAV on a small landing platform in an aquatic environment. We proposed a new capture system for this task. The system is divided into a winch subsystem and a magnetic catcher. The specific catcher includes a magnets array and an aligning mechanism. As depicted in Fig. 1, when the magnetic catchers captures the metal block, the capture system establishes a connection between UAV and catcher before UAV touchdown. Compared to previous works, the proposed system enable the UAV to land on the same position, which means the UAV requires a small landing pad. By employing this system, we can easily implement a UAV array in a limited landing platform. In this paper, we analyzed the design principle of the aligning mechanism and also the feasibility of the catcher. An optimization problem is formulated to obtain a better layout of magnets to obtain a larger acceptable area formed by the magnets for the metal block. We relaxed the problem based on interpolation simulations of attraction force. Experiments are conducted both in indoor and outdoor environments based on different UAV platforms respectively. The results validate that the design can achieve a successful landing with a landing pad smaller than the size of the UAV.

The remainder of this paper is organized as follows. Section II introduces the proposed system design with details. Section III mainly states the analysis on the aligning mechanism design principle and an optimized problem is formulated to find a better layout of the magnets array. In Section IV, the attraction force simulation results are presented, which show the insights to handle the optimization problem. The experiments are introduced in section V, followed by the section of conclusions.

II. Proposed System Design

A. System Overview

The main works we implemented is an improvement on the tethered-UAV landing method. Instead of tethering the UAV all the time, the proposed system only establishes a tether connection between the UAV and the platform when the UAV is about to land. To realize the system, we add a actuated winch to the UAV, as shown in Fig. 2. The winch system can release or retract a suspended metal block through a tether. Also, a magnetic catcher is designed for the landing platform to catch the metal block. We consider using the magnets to do the docking between the metal block and the magnetic catcher is because the magnets have an active attraction capability. The suspended metal block is actually the landing reference point once the connection is established. To make sure the landing point is fixed, an aligning mechanism is designed. The aligning mechanism can also be used to detach the metal block so that the UAV can take off again from the catcher.

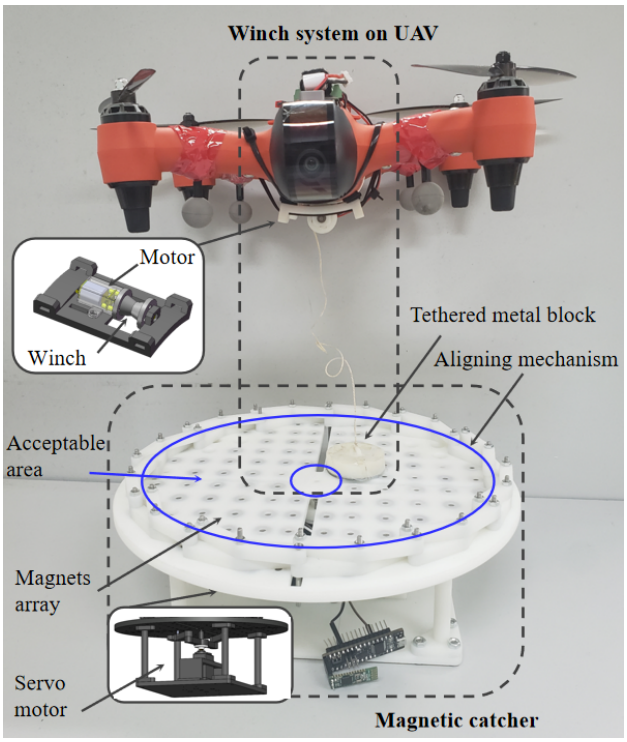

Fig. 2. System overview. The proposed capture system consists of two dashed parts in the figure.

B. Winch System

The winch system on UAV consists of a support base, a motor with a reducer, a winch and a tethered metal block. The winch system can be easily strapped to the abdomen of various UAVs and it is responsible for two tasks. First, the winch system releases the metal block which is like a "decoy" to the magnetic catcher to establish a connection. Second, it is also provides the driving forces to enable UAV declining until touching down the landing pad.

C. Proposed Magnetic Catcher

As shown in Fig. 2, the catcher mainly includes a magnets array, a circular support base with four sliding slots, an aligning linkage mechanism, and one servo motor. The magnets are evenly distributed on a support base to form a magnetic attraction area. The support base's surface is flat that a metal block can move on such a surface without obstruction. The aligning linkage mechanism which shows a ring-like shape is symmetrically placed near the edge of the base. Once a metal block enters into the vicinity of this magnetic area, it would be attracted firmly. Afterward, the aligning mechanism would start to shrink into a reduced state. This is an alignment process in which the metal block would be forced to move to the center of the support base.

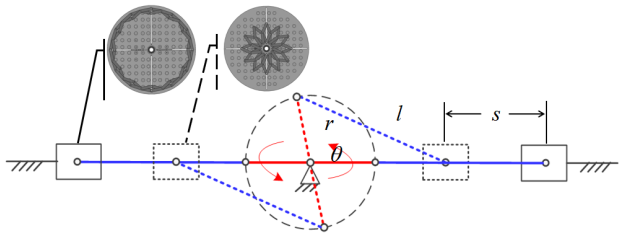

Fig. 3. Diagram of system driving method based on a centric double crank-slider mechanism. The solid line in the figure is initial expanded state. The dotted line implies a minimum state after a certain rotation motion, as the red arrows show.

1) Aligning Linkage Mechanism: The aligning linkage mechanism in our design looks like but not a regular polygon. It is a circular planar scissor structural mechanisms [21], which is deployable and can be folded. Similar structures can be found on the Puffetbot [22], where the researchers employ a similar design to protect a drone. The linkage mechanism can shrink or expand freely is very important for our design. We use the aligning attribute that the center of such a expanded structure will not change during the expand or shrink operations. The initial contact area between the metal block and the catcher is random in each time, while with the help of the aligning mechanism, the metal block will finally locates in the center of the support base. The metal block would be clamped by the aligning linkage mechanism because of the clamping force from the servo motor. Afterward, the winch system starts to work to force the UAV to decline until touching down. When the UAV needs to detach with the magnetic catcher and take off again, the aligning mechanism starts to expand to unlock the metal block. Note that, in the center area of the support base, no magnets are mounted, as the smaller blue circle shows in Fig. 2, this is deliberately designed to ensure the metal block can detach with the catcher.

2) Double Centric Crank-slider: In this design, the driving forces of alignment originated from the servo motor and transmit through a double centric crank-slider mechanism. The double centric crank-slider mechanism can balance the force act on both sides of the aligning linkage mechanism when it needs to shrink or expand. As shown in Fig. 3, the connecting rods represented by the blue lines are in a horizontal state, and the linkage mechanism is fully expanded. As the crank represented by the red line rotates, the two sliders which is the rectangles in the figure, move closer to each other. Thus, the aligning linkage mechanism starts to shrink to a minimum state. Suppose that the slider's stroke is s, the radius of the rotating crank is r, and the length of connecting rod is l. Then the angle that the crank needs to turn is obtained, as Equation (1) shows.

$$\theta = \frac{r^2 + (l - s + r)^2 - l^2}{2r(l - s + r)} \tag{1}$$

3) Acceptable Area: As for the catcher, all the magnets are embedded into the support base. Thus an attraction area is formed. The acceptable area is the area that could offer enough magnetic force to keep attracting the suspended metal block, as the blue circle shows in Fig. 2. With the different layout of magnets, for instance, various sizes of magnets, various distances between magnets, or various sizes of support base, the acceptable area could be different.

III. Analysis

A. Design Principle of Aligning Mechanism

The aligning mechanism in the catcher is composed of multiple angulated links [21]. All the angulated links are the same with an angle of w. The links $A_1C_1B_1$ and $A_1C_1B_1$ are connected by their respective midpoints C_1,C_2, as shown in Fig. 4, forming a basic unit of the aligning linkage mechanism. During alignment, the angle $\angle A_1CA_2$ keeps the same of a constant φ. To ensure multiple units can finally form a circle, this angle φ can be divisible by 2π. This can be written that

$$2\pi = N \cdot \varphi = N \cdot (\pi - \omega) \tag{2}$$

where N is the sides number of a regular polygon. The t is the length of $\overline{A_1B_2}$, it will change during the alignment. Using the law of sines in the triangle $\triangle A_1C_1(C_2)B_1$, the length of $\overline{A_1C_1(C_2)}$ can be calculated as

$$a = t\frac{\sin\phi}{\sin\mu} = t\frac{\sin\phi}{\sin(\pi - 2\phi)} \tag{3}$$

similarly, the length of $\overline{OB_2}$ can be further calculated in terms of the triangle $\triangle OB_2C_1(C_2)$ as

$$b = a\frac{\sin\left(\frac{\omega-\mu}{2}\right)}{\sin\left(\frac{\varphi}{2}\right)} \tag{4}$$

Based on the equations above, the feasibility condition of the alignment motion and the length relationships of the aligning linkage mechanism are presented. Generally, the more sides (a greater integer of N) a regular polygon has, its shape will be more closer to a circle. Therefore, an aligning mechanism with more connecting rods is more conducive to the aligning operation. But, in the meanwhile, more links will also increase the difficulties for assembly and smooth motion. These need to take into consideration when we try to build a prototype of aligning mechanism.

B. Analysis on Magnets Array

1) Prerequisites: In the catcher design, for a reasonable magnet array layout, it needs to meet two prerequisites. First, when the suspended metal block is attracted, the aligning mechanism should be able to force the metal block to push it to the center of the support base. Second, during the whole process of aligning, the metal block should be attracted all the time including the UAV declining process until touching down. Assuming that the maximum lift force of the UAV in disturbed environment is F_{max}, the friction coefficient between the metal block and support base is u, the attracted force acting on the metal block is F_a, and the thrusting force

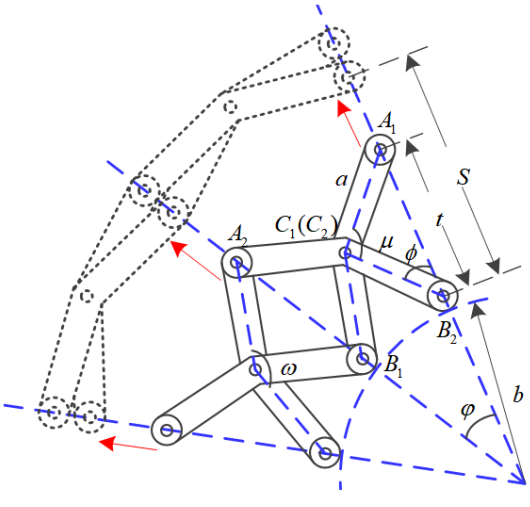

Fig. 4. Schematic diagram of the length and angle relationship of the basic units of aligning mechanism. The trajectory of the end points of each link during a expansion process are along the radius of the same circle, as the blue dotted lines show.

for alignment is F_p, the two conditions can be expressed as Equation (5) and Equation (6), respectively.

$$F_{a_{min}} > F_{max} \tag{5}$$

$$F_p > uF_a \tag{6}$$

Theoretically, the two conditions are easy to satisfy because we can use magnets with large enough size to provide with large enough attraction force F_a and also large enough motor with large thrusting force F_p.

2) Design optimization: By using different sizes of magnets, different quantities of magnets, and different motors, the total mass and the size of the magnetic catcher can be completely different. As for such a practical problem, we take the layout of magnets and the total mass into consideration to optimize the design of the catcher. This will be more accessible for the practical application scenarios that prefer less mass.

The magnets are evenly distributed and they form a a linear array in the support base. Suppose that the support base is much larger compared with each magnet, then the magnets array can be treated as a combination of the unit which is a square area, and four magnets are located at the vertices of the square unit, as shown in Fig. 5. The force acting on an object in the magnetic area has a great relationship with magnet size, magnet thickness, and distance between magnets. Aiming at the goal of obtaining an acceptable area as large as possible for the metal block under a limited total mass and considering such a magnets distribution, an approximate optimization problem can be formulated as Equation 7.

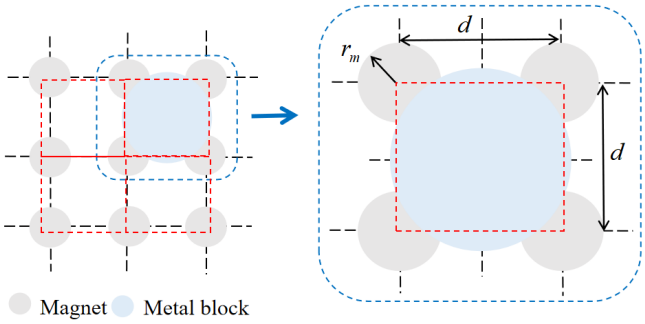

Fig. 5. Schematic diagram of a metal block located above four magnets. Left: a simplified diagram for magnets array distribution. Right: an enlarged view of a square unit.

$$\begin{aligned} \max_{r_m,h_m,d} \quad & S_a \\ s.t. \quad & 2r_m < d \\ & F_{max} < f(r_m, h_m, d) \\ & \tfrac{m_t}{S_a} = p_s * h_s + \tfrac{(\pi * r_m^2 (p_m - p_s) * h_m)}{d^2} \\ & h_m \leq h_s \end{aligned} \tag{7}$$

where S_a denotes the acceptable area, r_m is the radius of each magnet, d denotes the distance between each two magnets, m_t means total mass. The density of support base and magnet are p_s and p_m respectively. This is an approximated model compare to the real design because we ignore the edges and four slots in the support base. For the constraints in Equation 7, the first one means that there is no overlap between the magnets. Function $f(r_m, h_m, d_m)$ implies the corresponding magnet attraction force with respect to various parameters. The second constraint means the maximum lift force should be less than the attraction force. The $\frac{m_t}{S_a}$ is the aera density and it is obtained based on the idea that the area density of each square unit will change when magnets are embedded into the support base. For our design, if we want to keep the metal block be attracted all the time, we need to change the gap d, using different radius r_m or heights of magnets h_m.

IV. Simulation

The previous optimization problem is complicated because it is hard to get the accurate analytical expression of function $f(r_m, h_m, d)$ [23]. However, it can be simplified by fixing one parameter firstly combing some empirical results. For instance, the thickness of our support base h_s can not be too thin. Otherwise, it will deform easily. We use 3D printing to make the prototype with material of ABS, so we let the thickness h_s be no less than $6mm$. Also, to facilitate the installation of magnets, we let the height of a magnet (we use uniform magnets here) be not higher than the base's thickness so that we can embed the magnet into the support base. Once the thickness of magnet is fixed, the function $f(r_m, h_m, d)$ then is relaxed to $f(r_m, d)$. Thus, we can obtain the relationship based on interpolation

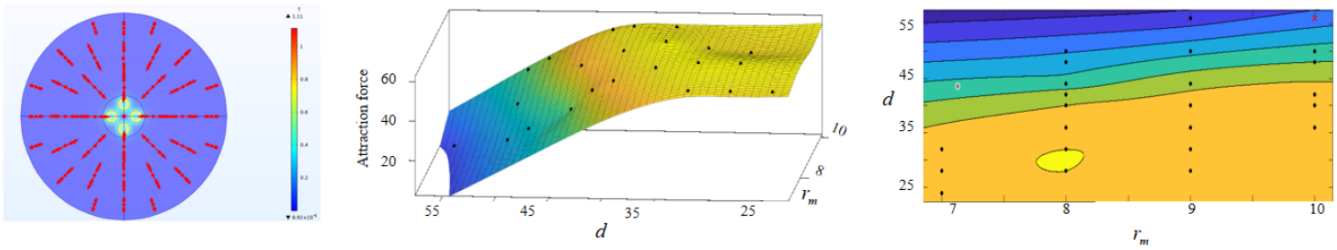

Fig. 6. Left: View of simulation model in Comsol Multiphysics. The red arrows denote the direction of magnetic field. The four circles in the center area represent four magnets, and overlapped by the metal block. Middle: Interpolation and fitting results of attraction force with differnet values of d and r_m. Right: Attraction force contour plot. r_m and d_m under a lower bound value of attraction force $30N$.

method. According to the square unit in Fig. 5, we build the corresponding simulation model in Comsol Multiphysics 5.5, as depicted in the left view of Fig. 6. In the simulations, we fix the h_m value to be $5mm$, and we choose N35 type magnets. Thus, based on the simulation model, we can obtain the force value under different values of r_m and d. Then the 3D fitting results is obtained and presented, as shown in the middle view of Fig. 6. The right view is a corresponding contour plot of the fitting results. We can further obtain the force relationship between r_m and d. For instance, if we want to generate the same attraction force, the distance d should set close to $35mm$ for magnets with a radius of $7mm$, and the distance can be set about to $40mm$ for magnets with a radius of $8mm$.

V. Experiments

A. Experiment Setup

Agree with the design principle and simulation results, a prototype of magnetic catcher has been made to validate the design, analysis and further explore the effectiveness and superiority of the proposed system. The employed magnets N35 in the design are both selected from off-the-shelf products. All design-related parameters are listed in Table I.

Experiments are conducted both in indoor and outdoor environments. An Optical Track motion capture (Mo-Cap) system, which provides us with poses information, is employed in the indoor experiment. We fixed the magnetic catcher on a shaking platform with one Degree of Freedom (1-DoF) to mainly test capture effect under a given disturbance. The outdoor experiments are mainly designed to test the system in a real-world environment. We also demonstrated our proposed envision in Fig. 1. The ESP32 controllers with onboard WIFI and Bluetooth functions are used as the winch system controller and magnetic catcher controller. With the wireless communication capability, it can transmit commands and information freely between the UAV, the catcher and users.

B. Indoor Experiment

In this experiment, the vibration was generated by the 1-DoF rotary platform. This platform can generate the motions given by users. An AR Drone 2.0 is used because of its ease of deployment. The winch system is attached to the bottom

TABLE I
DESIGN PARAMETERS OF PROTOTYPES

Parameters	***Value***
Total links of aligning linkage n_{link}	24
Radius of N35 magnets r_m	$5mm$
Distance of N35 magnets d	$29mm$
Height of N35 magnets h_m	$5mm$
F_{max}	$30N$
Height of support base h_s	$6mm$
Density of ABS p_s	$1.1g/cm^3$
Density of N35 magnets p_m	$7.5g/cm^3$

of the drone and shares the same battery with the drone. Based on the IMU data (with roll angle nears to 10 degrees) we collected from Qixing Bay, Shenzhen, China, we make the platform follow a sine wave motion with an amplitude of 10 degrees. Markers are attached to the UAV, metal block, and shaking platform. We use white paper to cover some noise in the Mo-Cap system for the shaking platform. Fig. 7 are the sequence views that illustrate the landing process including the UAV approaching, declining, and touchdown to the platform. Fig. 9 depicts heights changes of each object during a whole landing test. We can see from the enlarged view, the heights changes of the metal block become weak and follows the trend with the platform, this means the metal block has connected with the catcher. Hidden metal block in this figure means the metal block is in a unreleased state which can not de detected by the Mo-cap system. Thus, the values indcated by the magenta dashed line are estimated.

Fig. 7. Sequence views of UAV landing on 1-DoF shaking platform until it touches down.

C. Outdoor Experiment

In this experiment, the magnetic catcher is mounted on the surface of a multiple-UAVs landing platform. As shown

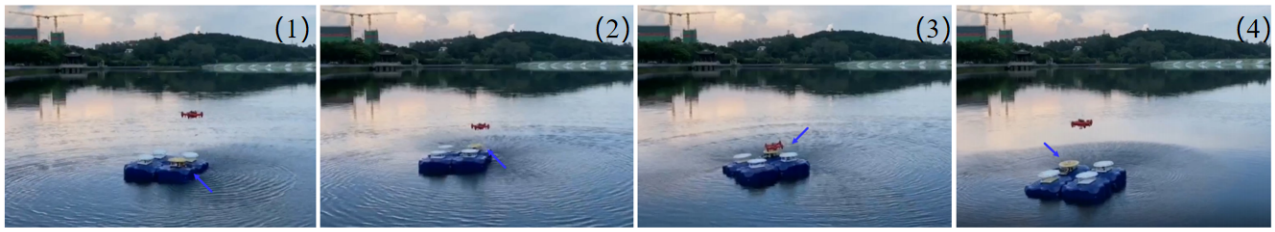

Fig. 8. From left to right: sequence views of a UAV landprocess, approaching, declining, touchdown, and re-takeoff.

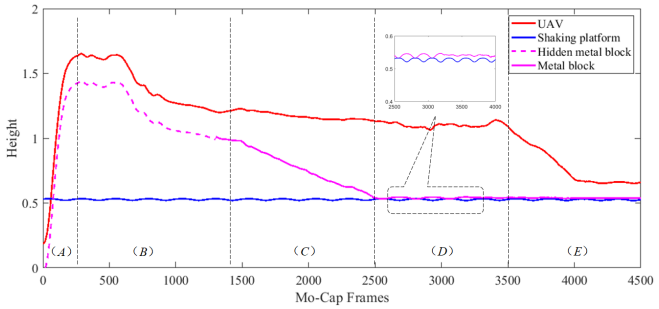

Fig. 9. Heights changes of each object during a landing test. From (A) to (E): UAV take-off, UAV approaches, releasing down the metal block and it attaches to catcher, touchdown.

TABLE II
PLANAR SIZE OF PROTOTYPES

Specifications	***Size***
Multiple-UAVs landing platform	$1m$ times $1m$
Magnetic catcher	Diameter is $260mm$
UAV with rotors	$340mm$ times $350mm$

in Fig. 8, a $2X2$ magnetic catcher array locates on a freely floating landing platform, and the UAV performs a successful landing from approaching to re-takeoff. From the subgraphs of Fig. 8, we find that the landing platform has rotated and moved during the landing, but they have no effect on the UAV landing. For this UAV landing test shows in the figure, the blue arrow indicates the corresponding catcher, which has a slight yellow color compared to the other three catchers. The planar size relationship among the catcher, UAV, and the mutliple-UAVs landing platform in this experiment is shown in Table. II.

VI. Comparison

The precise landing of UAV enable UAVs can be applied to many application scenarios, especially those when the space of landing pad is limited. However, according to the sate-of-the-art research, a precise UAV landing still requires a landing pad which is larger than the planar size of the UAV itself. The proposed approach in this paper can completely solve this problem, since our proposed solution can ensure that the touchdown point of UAV is a fixed point, which is the center of the magnetic catcher.

Moreover, our solution can also lock the drone. As mentioned, for tracking methods, like vision-guided UAV landing, there is no guarantee that the landing point will be the same every time due to the control algorithm can hardly deal with the random disturbance. Utilizing perching mechanism can also be treated as a special kind of UAV landing approach, but in fact the determination of the perching point is also based on a tracking algorithm, the same problem also occurs on the method that with the helf of a positioning mechanism for precise UAV landing. The detailed comparison between the mentioned methods is shown in Table. III.

TABLE III
PLANAR SIZE OF PROTOTYPES

Landing methods	***Fixed-point landing***	***Flight range***	***Landing pad***	***Reference***
Proposed system	**Yes**	No affect	Horizontal	
Vision-tracking	No	No affect	Horizontal	[13-15]
Perching mechanism	No	No affect	No Limits	[7-10]
Positioning mechanism	No	No affect	Horizontal	[6]
Tethered-UAV	Yes	Affected	Horizontal	[18-20]

VII. Conclusions and Future Work

In this paper, a precise landing of a UAV in an aquatic environment is presented based on the proposed capture system. This system offers the UAV a relative reference point for UAV landing. Also, the capture system provides the driving forces for UAV declining before touchdown. We presented the design guideline based on the geometric analysis of the aligning mechanism and the optimization view of the layout of the magnets. Real-world experimental results validate the feasibility of our proposed capture system. Because of the less landing space requirements, the biggest advantage of using this system is that it will be easy to deploy a UAV array in a landing platform with limited space. Therefore, we easily implement a UAV array in a limited space, we can deploy a UAV on a buoy while the landing pad will not occupy much space for the solar panels. For future work, we will consider more tests on the heavier external disturbance. More studies and optimizations on system design such as a reasonable length of the tether will be implemented to further enhance the system.

REFERENCES

[1] M. Maier and K. Kondak, "Landing of vtol uavs using a stationary robot manipulator: A new approach for coordinated control," in *2015 54th IEEE Conference on Decision and Control (CDC)*. IEEE, 2015, pp. 1497–1502.

[2] M. Lindemuth, R. Murphy, E. Steimle, W. Armitage, K. Dreger, T. Elliot, M. Hall, D. Kalyadin, J. Kramer, M. Palankar *et al.*, "Sea robot-assisted inspection," *IEEE robotics & automation magazine*, vol. 18, no. 2, pp. 96–107, 2011.

[3] X. Xiao, J. Dufek, T. Woodbury, and R. Murphy, "Uav assisted usv visual navigation for marine mass casualty incident response," in *2017 IEEE/RSJ International Conference on Intelligent Robots and Systems (IROS)*. IEEE, 2017, pp. 6105–6110.

[4] K. A. Talke, M. De Oliveira, and T. Bewley, "Catenary tether shape analysis for a uav-usv team," in *2018 IEEE/RSJ International Conference on Intelligent Robots and Systems (IROS)*. IEEE, 2018, pp. 7803–7809.

[5] T. Miki, P. Khrapchenkov, and K. Hori, "Uav/ugv autonomous cooperation: Uav assists ugv to climb a cliff by attaching a tether," in *2019 International Conference on Robotics and Automation (ICRA)*. IEEE, 2019, pp. 8041–8047.

[6] M. Galimov, R. Fedorenko, and A. Klimchik, "Uav positioning mechanisms in landing stations: Classification and engineering design review," *Sensors*, vol. 20, no. 13, p. 3648, 2020.

[7] K. Hang, X. Lyu, H. Song, J. A. Stork, A. M. Dollar, D. Kragic, and F. Zhang, "Perching and resting—a paradigm for uav maneuvering with modularized landing gears," *Science Robotics*, vol. 4, no. 28, p. eaau6637, 2019.

[8] H.-N. Nguyen, R. Siddall, B. Stephens, A. Navarro-Rubio, and M. Kovač, "A passively adaptive microspine grapple for robust, controllable perching," in *2019 2nd IEEE International Conference on Soft Robotics (RoboSoft)*. IEEE, 2019, pp. 80–87.

[9] L. Daler, A. Klaptocz, A. Briod, M. Sitti, and D. Floreano, "A perching mechanism for flying robots using a fibre-based adhesive," in *2013 IEEE International Conference on Robotics and Automation*. IEEE, 2013, pp. 4433–4438.

[10] Z. Huang, S. Li, J. Jiang, Y. Wu, L. Yang, and Y. Zhang, "Biomimetic flip-and-flap strategy of flying objects for perching on inclined surfaces," *IEEE Robotics and Automation Letters*, vol. 6, no. 3, pp. 5199–5206, 2021.

[19] M. Tognon, S. S. Dash, and A. Franchi, "Observer-based control of position and tension for an aerial robot tethered to a moving platform," *IEEE Robotics and Automation Letters*, vol. 1, no. 2, pp. 732–737, 2016.

[11] J. S. Wynn and T. W. McLain, "Visual servoing with feed-forward for precision shipboard landing of an autonomous multirotor," in *2019 American Control Conference (ACC)*. IEEE, 2019, pp. 3928–3935.

[12] M. Tognon, A. Testa, E. Rossi, and A. Franchi, "Takeoff and landing on slopes via inclined hovering with a tethered aerial robot," in *2016 IEEE/RSJ International Conference on Intelligent Robots and Systems (IROS)*, 2016, pp. 1702–1707.

[13] H. Lee, S. Jung, and D. H. Shim, "Vision-based uav landing on the moving vehicle," in *2016 International conference on unmanned aircraft systems (ICUAS)*. IEEE, 2016, pp. 1–7.

[14] A. Mohammadi, Y. Feng, C. Zhang, S. Rawashdeh, and S. Baek, "Vision-based autonomous landing using an mpc-controlled micro uav on a moving platform," in *2020 International Conference on Unmanned Aircraft Systems (ICUAS)*. IEEE, 2020, pp. 771–780.

[15] D. Hashemi and H. Heidari, "Trajectory planning of quadrotor uav with maximum payload and minimum oscillation of suspended load using optimal control," *Journal of Intelligent & Robotic Systems*, pp. 1–13, 2020.

[16] A. Paris, B. T. Lopez, and J. P. How, "Dynamic landing of an autonomous quadrotor on a moving platform in turbulent wind conditions," in *2020 IEEE International Conference on Robotics and Automation (ICRA)*. IEEE, 2020, pp. 9577–9583.

[17] L. Qian, S. Graham, and H. H.-T. Liu, "Guidance and control law design for a slung payload in autonomous landing: A drone delivery case study," *IEEE/ASME Transactions on Mechatronics*, vol. 25, no. 4, pp. 1773–1782, 2020.

[18] S.-R. Oh, K. Pathak, S. K. Agrawal, H. R. Pota, and M. Garrett, "Autonomous helicopter landing on a moving platform using a tether," in *Proceedings of the 2005 IEEE International Conference on Robotics and Automation*. IEEE, 2005, pp. 3960–3965.

[20] L. A. Sandino, D. Santamaria, M. Bejar, A. Viguria, K. Kondak, and A. Ollero, "Tether-guided landing of unmanned helicopters without gps sensors," in *2014 IEEE International Conference on Robotics and Automation (ICRA)*. IEEE, 2014, pp. 3096–3101.

[21] F. Maden, K. Korkmaz, and Y. Akgün, "A review of planar scissor structural mechanisms: geometric principles and design methods," *Architectural Science Review*, vol. 54, no. 3, pp. 246–257, 2011.

[22] H. Hedayati, R. Suzuki, D. Leithinger, and D. Szafir, "Pufferbot: Actuated expandable structures for aerial robots," in *2020 IEEE/RSJ International Conference on Intelligent Robots and Systems (IROS)*. IEEE, 2020, pp. 1338–1343.

[23] D. Vokoun, G. Tomassetti, M. Beleggia, and I. Stachiv, "Magnetic forces between arrays of cylindrical permanent magnets," *Journal of Magnetism and Magnetic Materials*, vol. 323, no. 1, pp. 55–60, 2011.